

## Normal Operation Characteristics of 30kW Scale CVCF Inverter-Based Micro-grid System

Marito Ferreira, Hu-Dong Lee, Dong-Hyun Tae, Dae-Seok Rho\*  
Dept. of Electrical Engineering, Korea University of Technology and Education

### 30kW급 CVCF 인버터 기반의 Micro-grid의 정상상태 운용특성에 관한 연구

페레이라 마리토, 이후동, 태동현, 노대석\*  
한국기술교육대학교 전기공학과

**Abstract** Recently, for the purposes of reducing carbon dioxide(CO<sub>2</sub>) emissions in the island area, countermeasures to decrease the operation rate of diesel generator(DG) and to increase one of renewable energy sources(RES) is being studied. In particular, the demonstration and installation of stand-alone micro-grid(MG) system which is composed of DG, RES and energy storage system(ESS) has been implemented in some island areas such as Gapa-do, Gasa-do and Ulleung-do island. However, many power quality(PQ) problems may be occurred due to an intermittent output of RES including photovoltaic(PV) system and wind power(WP) system in a normal operating of constant voltage & constant frequency(CVCF) inverter-based MG system. Therefore, this paper presents a modeling of the 30kW scale MG system using PSCAD/EMTDC, and also implements a 30kW scale CVCF inverter-based MG system as test devices to analyze normal operating characteristics of MG system. From the simulation and test results, it is confirmed that the proposed methods are useful and practical tools to improve PQ problems such as under-voltage, over-voltage and unbalanced load in CVCF inverter-based MG system.

**요약** 최근, 국내외적으로 CO<sub>2</sub>배출의 저감을 위한 기술적인 방안 중 하나로 도서지역의 마이크로그리드에 기 설치된 디젤발전기의 가동률을 줄이고 신재생에너지전원의 비중을 높여 운용하고 있는 실정이다. 특히, 국내에서는 가파도, 가사도, 울릉도 등의 도서지역에 디젤발전기와 신재생에너지, 전기저장장치로 구성된 독립형 마이크로그리드의 실증 및 보급 사업이 활발하게 진행되고 있으며, 기존의 디젤발전기 대신 정전압, 정주파수(constant voltage constant frequency, CVCF) 기능을 가진 CVCF 인버터 및 CVCF 인버터용 배터리를 도입하여 마이크로그리드를 안정적으로 운용하는 연구들이 진행되고 있다. 그러나, CVCF 인버터 기반 마이크로그리드의 정상상태 운용특성에 있어서, 출력이 불안정한 태양광전원과 풍력발전과 같은 신재생에너지전원이 계통에 연계되면서 전력품질에 많은 문제가 발생하고 있다. 따라서, 본 논문에서는 신재생에너지전원과 전기저장장치 연계에 따른 마이크로그리드의 운용특성을 분석하기 위하여, PSCAD/EMTDC를 이용하여 30kW급 마이크로그리드 시스템을 모델링하고, 이를 바탕으로 마이크로그리드 시험장치를 구현한다. 30kW급 마이크로그리드 시스템을 바탕으로 시뮬레이션 및 시험을 수행한 결과, 제안한 방법이 CVCF 인버터 기반의 마이크로그리드 시스템에서 저전압, 과전압 및 불평형 문제를 개선하는 데 유용함을 확인하였다.

**Keywords** : Island Micro-grid System, Power Quality Characteristics, Normal Operation, CVCF Inverter, PSCAD/EMTDC

This work was supported by the Korea Institute of Energy Technology Evaluation and Planning(KETEP) and granted financial resources from the Ministry of Trade, Industry & Energy(No.20182410105070, No.20191210301940).

\*Corresponding Author : Dae-Seok Rho(Korea University of Technology and Education)  
email: dsrho@koreatech.ac.kr

Received May 13, 2020

Revised June 2, 2020

Accepted June 5, 2020

Published June 30, 2020

## 1. Introduction

These days, because the shortage of energy and environmental pollution issues has been widely emerging all over the world, the concerns of MG systems including RES and ESS are being increased[1-3]. In particular, the demonstration and installation of stand-alone MG systems which are composed of DG, RES and ESS have been implemented in some island areas such as Gapa-do, Gasa-do and Ulleung-do island[4]. However, in normal operating characteristics of CVCF inverter-based MG system, many PQ problems may be occurred due to variability and intermittency of output in RES[5,6]. And also, the fluctuation of RES may cause unstable operation in MG system. In other words, PQ problems and instability of the existing system may be caused by the rapid output fluctuation of RES which is highly affected by weather conditions. Therefore, this paper presents a modeling of the 30kW scale MG system using PSCAD/EMTDC. Furthermore, this paper implements a 30kW scale CVCF inverter-based MG system as test devices to perform normal operations of MG system. From the simulation and test results, it is confirmed that the proposed methods are useful and practical tools to improve PQ problems such as under-voltage, over-voltage and unbalanced load in CVCF inverter-based MG system.

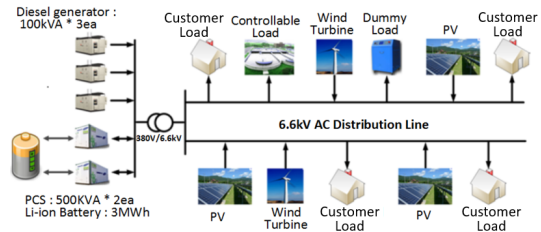


Fig. 1. Configuration of conventional island MG system

On the other hand, for the purposes of reducing CO<sub>2</sub>(carbon dioxide) emissions in the island area, countermeasures to decrease the operation rate of DG and to increase one of RES is being studied as shown in Fig. 2[9,10]. However, it is reported that in normal operating characteristics of CVCF inverter-based MG system, a phenomenon of under-voltage may be occurred, if output capacity of the customer load is larger than PV system. Contrary, if the output capacity of PV system is larger than the customer load, a phenomenon of over-voltage is happened due to the voltage rising which is influenced by the reverse power flow of PV system. And also, an unbalanced voltage in MG system is mostly caused by varied unbalanced load and line impedance. Besides, although an unbalanced load rate is greatly increased in MG system, CVCF inverter should be operated in a normal condition without shutting down.

## 2. Operation characteristics of 30kW CVCF inverter-based MG system

Generally, stand-alone MG systems in island areas are composed of diesel generator, RES, ESS, and customer loads which are conventionally demonstrated as shown in Fig. 1. Here, diesel generator and RES supply power to customer load in normal operation, while ESS performs various operation functions such as load control and output stabilization of RES[7,8].

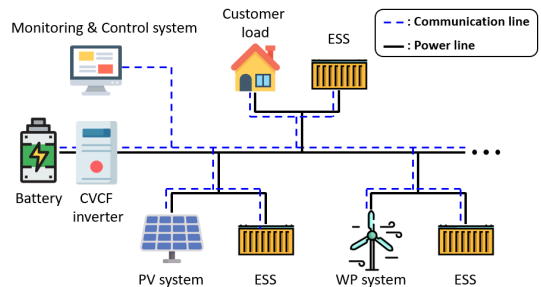


Fig. 2. Configuration of CVCF inverter-based MG system

### 3. Modeling of 30kW CVCF inverter-based MG system based on PSCAD/EMTDC

#### 3.1 CVCF inverter modeling

The CVCF inverter is usually designed to reduce an error of target voltage and accelerate the response characteristics using a PI (proportional-integral) control algorithm, which can be expressed as shown in Eq. (1). Here, the first term of Eq. (1) calculates a proportional control signal with the difference between target voltage ( $V_{ac-ref}$ ) and output voltage ( $V(t)$ ), the second term accumulates an error to obtain an integral control signal to determine waveform, frequency, and phase of target voltage.

$$Wave_{ref} = \left[ K_p \left( 1 - \frac{V(t)}{V_{ac-ref}} \right) + K_i \int_0^t \left( 1 - \frac{V(\tau)}{V_{ac-ref}} \right) d\tau \right] \cdot \sin(2\pi ft + \phi) \quad (1)$$

Where,  $Wave_{ref}(t)$  : reference waveform,  $K_p$  : proportional factor,  $K_i$  : integral coefficient,  $V(t)$ : output voltage,  $V_{ref}$  : target voltage.

Based on the above Eq. (1) to obtain a reference waveform, the modeling of CVCF inverter is performed by using PSCAD/EMTDC, as shown in Fig. 3. Here, section A calculates an error value by comparing target voltage with output voltage, section B is a PI control for each error value, section C determines waveform, frequency, and phase of target voltage. Furthermore, section D shows an output of carrier to triangular wave, section E indicates a signal of comparator between a reference wave and carrier wave, which is converted into a PWM signal.

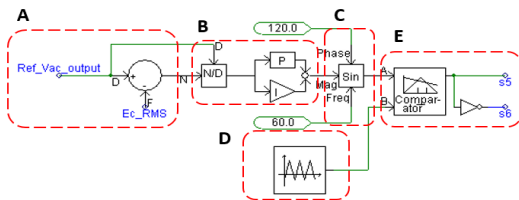


Fig. 3. Modeling of voltage and frequency control in CVCF inverter

Furthermore, the modeling of CVCF inverter with IGBT(insulate gate bipolar transistor) is driven by six switching signals from PWM and converts a DC input of the battery into a three-phase AC output with a different phase of  $120^\circ$ , as shown in Fig. 4.

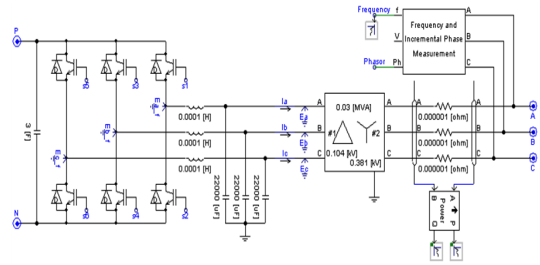


Fig. 4. Modeling of CVCF inverter

#### 3.2 PV system modeling

The desired instantaneous active power(P) and reactive power(Q) of PV system are generally determined by d-q axis variables that are converted to DC power from 3-phase AC power based on the stationary and synchronous coordination system. In other words, instantaneous active power and reactive power in a 3-phase balanced system, which can be expressed as shown in Eq. (2) based on the concept of the d-q coordinate method. And the output voltage of  $V_d$  in d-q axis rotating at synchronous speed is equal to the instantaneous voltage magnitude of the output terminal. And also, the output voltage of  $V_q$  is 0, as shown in Eq. (3), which can be obtained from Eq. (2).

$$P = \frac{3}{2}(V_d I_d + V_q I_q), \quad Q = \frac{3}{2}(V_d I_q - V_q I_d) \quad (2)$$

$$P = \frac{3}{2} |V_0| I_q, \quad Q = -\frac{3}{2} |V_0| I_d \quad (3)$$

Where,  $V_d, V_q$ : output voltages of the d-axis and q-axis,  $I_d, I_q$ : output currents of d-axis and q-axis,  $|V_0|$ : magnitude of instantaneous voltage.

Here, in order to control the desired active and reactive power of grid-connected inverter of PV system, current control algorithms with a PI controller which can be expressed, as shown in Eq. (4) and Eq. (5). In this process, the active and reactive power of PV system can be controlled in an independent manner, because there is a decoupling circuit in a current control equation.

$$V_{d-ref} = (I_{d-ref} - I_d) \cdot (k_p + \frac{k_i}{s}) - I_q \cdot \omega L + V_{sq} \quad (4)$$

$$V_{q-ref} = (I_{q-ref} - I_q) \cdot (k_p + \frac{k_i}{s}) + I_d \cdot \omega L \quad (5)$$

As mentioned above Eq. (4) and Eq. (5), the modeling of a PI current control is performed by using PSCAD/EMTDC, as shown in Fig. 5. Here, Fig. 5(a) shows a current control modeling in a q-axis and Fig. 5(b) represents a current control modeling in d-axis.

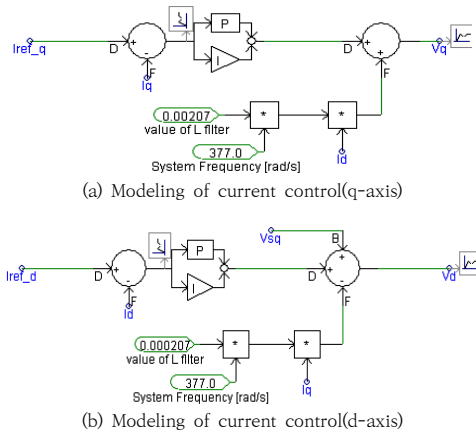


Fig. 5. Modeling of current control in PV system

Furthermore, modeling of the grid-connected inverter of PV system with IGBT is driven by six switching signals from PWM and convert to output DC which generated PV system into three-phase output AC with a different phase of  $120^\circ$ , as shown in Fig. 6.

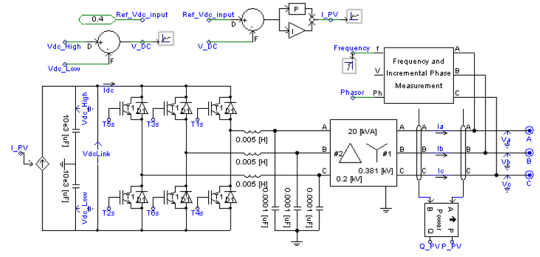


Fig. 6. Modeling of grid-connected inverter in PV system

### 3.3 Customer load modeling

The modeling of artificial customer loads which are composed of reactance, inductance, and capacitance with the characteristic of constant impedance(Z). Here, the resistance component is adjusted by 100[W] unit from 100 to 10,000[W]. And also, the capacitive and inductive components are adjusted by 100[Var] unit from 100 to 10,000[Var]. Furthermore, the power factor is adjusted by using an inductive load and capacitive loads, which are illustrated, as shown in Fig. 7.

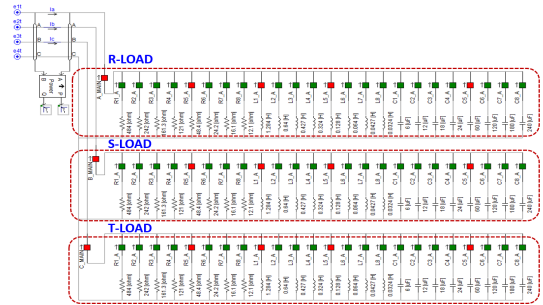


Fig. 7. Modeling of customer load

### 3.4 Entire system modeling

Based on the proposed modeling as mentioned earlier in order to maintain a constant voltage and constant frequency in MG system, this paper performs an entire modeling of 30kW CVCF inverter-based MG system, which can be illustrated as shown in Fig. 8. Here, the entire modeling is composed of 30kW CVCF inverter, 20[kWh] Li-ion battery, 20[kW] PV system, and 30[kW] customer loads.

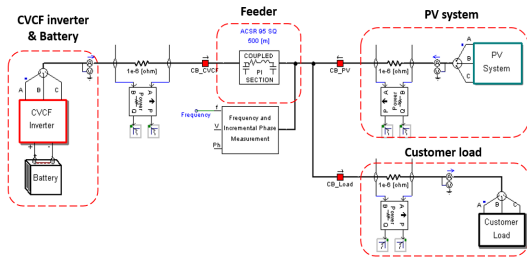


Fig. 8. Modeling of entire system

## 4. Implementation of 30kW CVCF inverter-based MG system

### 4.1 CVCF inverter

The hardware system of CVCF inverter-based MG system is designed and implemented to receive power from DC battery and converted into AC power through IGBT components. And also, it adapts a PWM control method with a capacity of 30kW and the efficiency is more than 90%. Furthermore, it plays an important role to maintain a constant voltage and constant frequency in MG system. Table 1 shows the detailed specifications of 30kW CVCF inverter.

Table 1. Specification of CVCF inverter

items	specification standards	
inverter	control element	frequency switching microprocessor with PWM methods
	type	IGBT
	connection type	3 $\phi$ 4-wire with grounding
	rated voltage	380V
output	power factor	0.8
	voltage distortion	within 5%
	voltage stability	within $\pm 1\%$
	transient voltage fluctuation	within $\pm 5\%$ (100% of sudden load changing)
	transient response speed	within 50msec
	frequency stability	within 60HZ $\pm 0.1$ Hz
	voltage regulation range	within $\pm 10\%$

### 4.2 Artificial PV system

In order to design the output of an artificial

PV system same as a real distribution system, this paper implements an artificial PV system which can be illustrated, as shown in Fig. 9. Here, the artificial PV system is composed of 20[kVA] 3-phase inverter and 20[kW] DC power supply. And also, the output voltages of PV system are adjusted by varying DC currents.

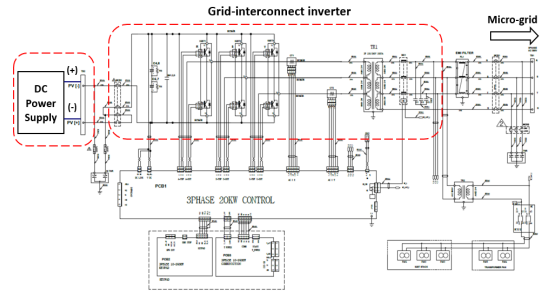


Fig. 9. Configuration of artificial PV system

### 4.3 Artificial customer load

The artificial customer loads are composed of reactance, inductance, and capacitance with the characteristic of constant impedance(Z). Here, the resistance component is adjusted by 100[W] unit from 100 to 10,000[W]. And also, capacitive and inductive components are adjusted by 100[Var] unit from 100 to 10,000[Var]. Furthermore, the power factor is adjusted based on the inductive load and capacitive loads, as shown in Fig. 10.

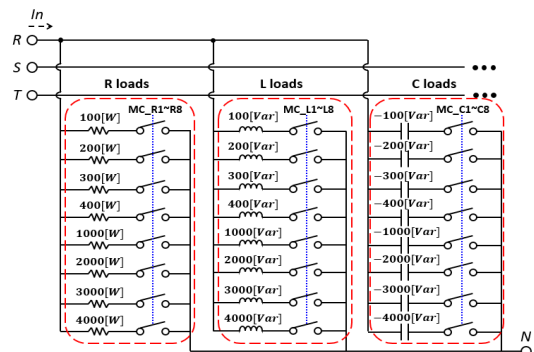


Fig. 10. Configuration of artificial customer load

### 4.4 Entire system

Based on the test devices as mentioned earlier in order to maintain a constant voltage and constant frequency, this paper implements a 30kW scale CVCF inverter-based MG system, which is illustrated as shown in Fig. 11. Here, the entire system is composed of 20[kW] Li-ion battery, CVCF inverter, 30[kW] artificial customer load and 20[kW] artificial PV system.

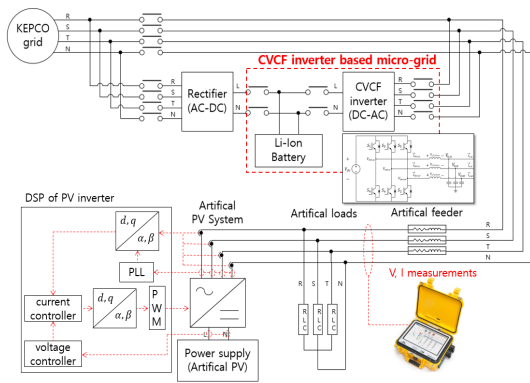


Fig. 11. Configuration of entire system

## 5. Case studies

### 5.1 Simulation and test conditions

In order to evaluate PQ characteristics such as under-voltage, over-voltage, and unbalanced load according to operating of CVCF inverter-based MG system, this paper assumes a simulation and test conditions of various PQ characteristics as shown in Table 2. Here, 1[kW], 1.5[kW], 3.5[kW] of customer loads and 3[kW], 6[kW], 9[kW], 12[kW] of PV system and 1.5[Ω] line impedance are assumed in case of under-voltage and over-voltage. And also, when 2.6[kW], 2[kW], 1.1[kW], 0.6[kW] of customer loads and 1.5[Ω] line impedance are assumed in case of an unbalanced load. Furthermore, 3 cases of unbalanced load rates are assumed as 38%, 86% and 129%.

Table 2. Simulation and test conditions of PQ

items	contents
under-voltage & over-voltage	<ul style="list-style-type: none"> <li>• capacity of customer loads: 1[kW], 1.5[kW] and 3.5[kW]</li> <li>• capacity of PV system: 3[kW], 6[kW], 9[kW] and 12[kW]</li> <li>• capacity of line impedance: 1.5[Ω]</li> </ul>
unbalanced load	<ul style="list-style-type: none"> <li>• 0% (R:2.6[kW], S:2.6[kW], T:2.6[kW])</li> <li>• 38% (R:2[kW], S:2.6[kW], T:2.6[kW])</li> <li>• 86% (R:1.1[kW], S:2.6[kW], T:2.6[kW])</li> <li>• 129% (R:0.6[kW],S:3.8[kW], T:3.8[kW])</li> </ul>

### 5.2 Operation characteristics of 30kW MG system using PSCAD/EMTDC

#### (1) Characteristics of under-voltage and overvoltage

In order to analyze PQ characteristics including under-voltage, over-voltage, and unbalanced load, this paper presents an operation characteristic of the CVCF inverter-based MG system using PSCAD/EMTDC. Here, when 1[kW] customer load and 1.5[Ω] line impedance are operated simultaneously in the MG system, customer voltage decreases from 220[V] to 212[V] due to voltage drop with the line impedances, which can be illustrated as shown in sections ① and ② of Fig. 12. And if customer load increases from 1.0[kW] to 1.5[kW], customer voltage decreases from 212[V] to 206[V] as shown in section ③ of Fig. 12. And also, if customer load increases from 1.5[kW] to 3.5[kW], customer voltage reduces from 206[V] to 194[V] as shown in section ④ of Fig. 12.

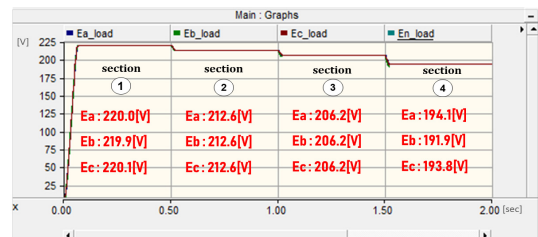


Fig. 12. Characteristics of under-voltage without PV system

Furthermore, when 3[kW] PV system and 1.5[Ω] line impedance are interconnected and operated in the MG system, PCC(power coupling common) voltages at PV system increases from 220[V] to 226[V] due to voltage rising with reverse power flow of PV system, which can be expressed as shown in sections ① and ② of Fig. 13. And if the capacity of PV system rises from 3[kW] to 6[kW], PCC voltage increases from 226[V] to 233[V] as shown in sections ③ of Fig. 13. And also, if the capacity of PV system increases from 6[kW] to 9[kW], PCC voltage increases from 233[V] to 239[V] as shown in section ④ of Fig. 13. However, once the capacity of PV system increases from 9[kW] to 12[kW], PCC voltage rises from 239[V] to 243[V], and then they cause shut-down phenomenon due to violating allowable maximum limit of grid-connected inverter in PV system, which is indicated as shown in case ⑤ of Fig. 13. From the simulation results, it is confirmed that the over-voltage phenomenon with reverse power flow of PV system may cause a shut-down of the grid-connected inverter.

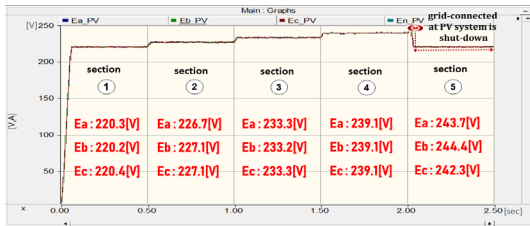


Fig. 13. Characteristics of over-voltage with PV system

(2) Characteristics of unbalanced load

In case of a balanced load 0% in Table 2, customer voltages at R, S, T phases decrease from 219[V] to 199[V] respectively, which is illustrated as shown in case ① of Fig. 14. And in the case of 38% unbalanced load rates, customer voltage of R phase increases from 199[V] to 204[V] and customer voltages of S, T phases are the same as shown in section ② of Fig. 14. And also, in case of 86% unbalanced load rates,

customer voltage of R phase increases from 204[V] to 212[V] and customer voltages of S, T phases are the same as shown in sections ③ of Fig. 14. Furthermore, in the case of 129% unbalanced load rates, customer voltage of R phase rises from 212[V] to 215[V] and customer voltages of S, T phases are the same which is indicated as shown in section ④ of Fig. 14. Therefore, it is confirmed that the CVCF inverter is operated in normal conditions, even though the unbalanced load rate is 129%.

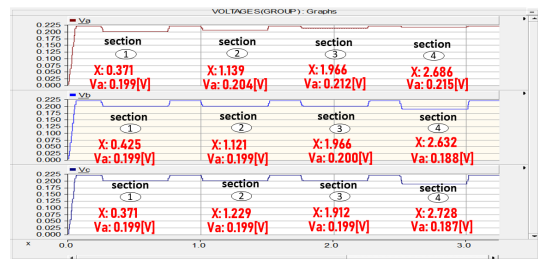


Fig. 14. Characteristics of unbalanced voltage without PV system

5.3 Operation characteristics of 30kW MG system with test devices

(1) Characteristics of under-voltage and overvoltage

In order to analyze PQ characteristics including under-voltage, over-voltage, and unbalanced load, this paper presents an operation characteristic of the CVCF inverter-based MG system based on the test devices. Here, when 1[kW] customer load and 1.5[Ω] line impedance are operated simultaneously in the MG system, customer voltage decreases from 219[V] to 212[V] due to voltage drop with the line impedances, which can be illustrated as shown in sections ① and ② of Fig. 15. And if customer load increases from 1.0[kW] to 1.5[kW], customer voltage decreases from 212[V] to 206[V] as shown in section ③ of Fig. 16. And also, if customer load increases from 1.5[kW] to 3.5[kW], customer voltage reduces from 206[V] to 196[V] as shown in section ④ of Fig. 15.

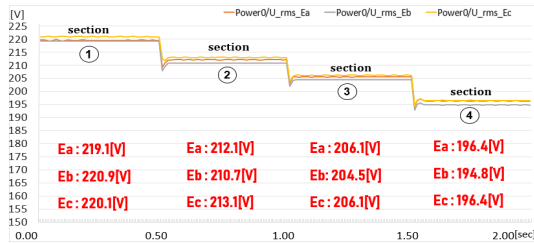


Fig. 15. Characteristics of under-voltage without PV system

Furthermore, when 3[kW] PV system and 1.5[Ω] line impedance are interconnected and operated in the MG system, PCC(power coupling common) voltages at PV system increases from 220[V] to 229[V] due to voltage rising with reverse power flow of PV system, which can be expressed as shown in sections ① and ② of Fig. 16. And if the capacity of PV system rises from 3[kW] to 6[kW] PCC voltage increases from 229[V] to 235[V] as shown in sections ③ of Fig. 16. And also, in case the capacity of PV system rises from 6[kW] to 9[kW], PCC voltage increases from 235[V] to 239[V] as shown in cases ④ of Fig. 16. However, once the capacity of PV system increases from 9[kW] to 12[kW], PCC voltage rises from 239[V] to 244[V], and then they cause shut-down phenomenon due to violating allowable maximum limit of grid-connected inverter in PV system, which is indicated as shown in case ⑤ of Fig. 16. From the test results, it is confirmed that the over-voltage phenomenon with reverse power flow of PV system may cause the shut-down of the grid-connected inverter.

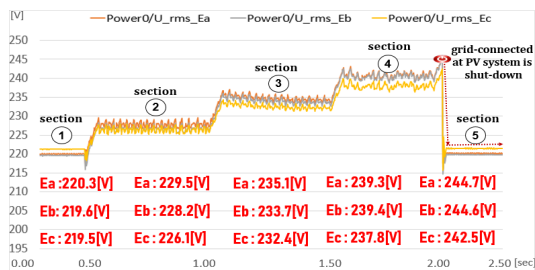


Fig. 16. Characteristics of over-voltage with PV system

## (2) Characteristics of unbalance load

In case of a balanced load 0% in Table 2, customer voltages at R, S, T phases decrease from 220[V] to 199[V] respectively, which is illustrated as shown in case ① of Fig. 17. And in case of 38% unbalanced load rates, customer voltage of R phase increases from 199[V] to 205[V] and customer voltages of S, T phases are the same as shown in section ② of Fig. 17. And also, in case of 86% unbalanced load rates, customer voltage of R phase increases from 205[V] to 215[V] and customer voltages of S, T phases are the same as shown in sections and ③ of Fig. 17. Furthermore, in the case of 129% unbalanced load rates, customer voltage of R phase rises from 215[V] to 219[V] and customer voltages of S, T phases are the same which is indicated as shown in section ④ of Fig. 17. Therefore, it is confirmed that the CVCF inverter is operated in normal conditions, even though the unbalanced load rate is 129%.

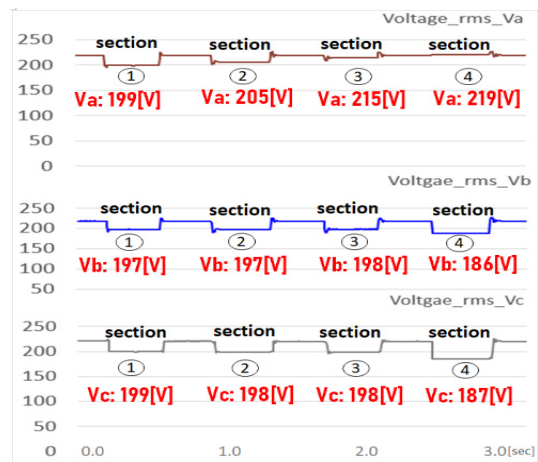


Fig. 17. Characteristics of unbalanced voltage without PV system

## 6. Conclusions

This paper has presented modeling of the 30kW scale MG system using PSCAD/EMTDC, and

also implemented a 30kW scale CVCF inverter-based MG system as test devices to analyze power quality problems such as under-voltage, over-voltage and unbalanced load in CVCF inverter-based MG system. The main results of this paper are summarized as follows.

- (1) With the increase of capacity in PV system, the grid-connected inverter may be shut-down due to violating allowable maximum limit, and then it is confirmed that the over-voltage phenomenon with reverse power flow of PV system may cause the shut-down of the grid-connected inverter.
- (2) It is found that the CVCF inverter is operated in normal conditions, even though the unbalanced load rate is 129% based on the test results.
- (3) As the simulation results are identical to test results, it is confirmed that the proposed method is useful to analyze power quality problems in CVCF inverter-based MG system.

## References

- [1] IEC white paper, "Microgrids for disaster preparedness and recovery with electricity continuity plans systems", originally published in March, 2014.
- [2] Kohn, Z. B. Zabinsky and A. Nerode, "A Micro-Grid Distributed Intelligent Control and Management System", IEEE Transactions on Smart Grid, vol. 6, no. 6, pp. 2964-2974, 2015.  
DOI: <https://doi.org/10.1109/TSG.2015.2455512>
- [3] Mohamad Faisal, M.A. Hannam, Pin Jern Ker, Aini Hussain, "Review of Storage system technology in microgrid application: Issues and challenges", IEEE Access Special section on advance energy storage technology and their applications, vol. 6, no. 6, pp. 35143-35164, 2018.  
DOI: <https://doi.org/10.1109/ACCESS.2018.2841407>
- [4] Dong-Wan Kim, Ji-Han Ko, Seong Hyun Kim, Homin Kim, "Renewable Energy Configuration Plan of Micro Grid in Gapa Island", Journal of the Korean Solar Energy Society, vol. 34, no. 2, pp. 16-32, 2014.  
DOI: <https://doi.org/10.7836/kses.2014.34.2.016>
- [5] M.S. Mahmoud, S. Azher Hussain, M.A.Abido, "Modeling and control of microgrid: An overview" Journal of the Franklin Institute, vol. 351. no. 5, pp. 2822-2859, 2014.  
DOI: <https://doi.org/10.1016/j.ifranklin.2014.01.016>
- [6] Vinayangam Arangarajan, Swarna KVS, Yong Sheon Khoo, Alex Stojcevski, "Power Quality Analysis in Microgrid: An Experimental Approach", Journal of Power and Energy Engineering, vol. 4, no. 4, 2016.  
DOI: <https://doi.org/10.7836/kses.2014.34.2.016>
- [7] Sung-Sik Choi, Min-Kwan Kang, Hu-Dong Lee, Yang-Hyun Nam, Dae-Seok Rho, "A stable Operation Strategy in Micro-grid Systems without Diesel Generators", Journal of Electric Engineering and Technology, vol. 13, no. 1, pp. 114~123, 2018.  
DOI: <http://doi.org/10.5370/JEET.2018.13.1.114>
- [8] B. V. Solanki, A. Raghurajan, K. Bhattacharya and C. A. Cañizares, "Including Smart Loads for Optimal Demand Response in Integrated Energy Management Systems for Isolated Microgrids", IEEE Transactions on Smart Grid, vol. 8, no. 4, pp. 1739-1748, 2017.  
DOI: <https://doi.org/10.1109/TSG.2015.2506152>
- [9] Woo-Hyun Hwang, Sang-Kyu Kim, Jung-Ho Lee, Woo-Kyu Chae, Je-Ho Lee, Hyun-Jun Lee, Jae-Eon Kim "Autonomous Micro-grid Design for Supplying Electricity in Carbon-Free Island", Journal of Electrical Engineering & Technology, vol. 9, no. 3, pp. 1112~1118, 2014.  
DOI: <http://dx.doi.org/10.5370/JEET.2014.9.3.1112>
- [10] Seung-Ho Kim, Sung-Sik Choi, Seung-Jong Kim, Dae-Seok Rho, "Single-phase Control Algorithm of 4-Leg type PCS for Micro-grid System", Korea Academy Industrial Cooperation Society, vol. 18, no. 11, pp. 817-825, 2017.  
DOI: <https://doi.org/10.5762/KAIS.2017.18.11.817>

---

## Marito Ferreira(페레이라 마리토) [Regular member]



- Nov. 2013 : National University of East Timor, Electrical Engineering, B.S
- Feb. 2018 : Korea University of Technology and Education, Electrical Engineering, M.S

• Sep. 2018 ~ current : Korea University of Technology and Education, Electrical Engineering, Ph.D. Student

### <Research Interests>

Power quality analysis, distribution system and energy storage system

Hu-Dong Lee(이 후 동) [Regular member]



- Aug. 2016 : Korea University of Technology and Education, Electrical Engineering, B.S
- Aug. 2018 : Korea University of Technology and Education, Electrical Engineering, M.S

- Sep. 2018 ~ current : Korea University of Technology and Education, Electrical Engineering, Ph.D. Student

⟨Research Interests⟩

Distribution system, power quality, coordination of protection devices, renewable energy sources and micro-grid

Dae-Seok Rho(노 대 석) [Regular member]



- Feb. 1985 : Korea University, Electrical Engineering, B.S
- Feb. 1987 : Korea University, Electrical Engineering, M.S
- Mar. 1997 : Electrical Engineering, Hokkaido University, Ph.D.

- Mar. 1987 ~ Aug. 1998 : Korea Electrotechnology Research Institute, senior researcher
- Mar. 1999 ~ current: Korea University of Technology and Education, Electrical Engineering, professor

⟨Research Interests⟩

Operation of power distribution systems, dispersed storage and generation systems and power quality

Dong-Hyun Tae(태 동 현) [Regular member]



- Aug. 2014 : Korea University of Technology and Education, Electrical Engineering, B.S
- Aug. 2016 : Korea University of Technology and Education, Electrical Engineering, M.S

- Sep. 2019 ~ current : Korea University of Technology and Education, Electrical Engineering, Ph.D. Student

⟨Research Interests⟩

Distribution system, power quality, energy storage system, renewable energy sources and micro-grid